Superhydrophobic Coating of European Oak (*Quercus robur*), European Larch (*Larix decidua*), and Scots Pine (*Pinus sylvestris*) Wood Surfaces

Václav Šprdlík,[a,*] Veronika Kotradyová,[b] and Radovan Tiňo [c]

Plant surfaces provide an unlimited source of systems for the protection of their surface against the outer environment. These systems have continuously improved over the last 400 million years of evolution. Two of the most fascinating properties of these systems are superhydrophobicity and the self-cleaning ability of several plant species. These properties are most often achieved due to the hierarchical structure of the surface in combination with a deposited blend of epicuticular waxes. In this study, a layer of n-hexatriacontane was deposited on wood surfaces *via* thermal evaporation, and the self-assembly ability was investigated for various wood species with differently machined surfaces. The behavior of wax crystals was observed using scanning electron microscopy (SEM) and confocal microscopy. The impact on wettability was investigated by measuring contact angles and tilt angles. With wax deposition, a significant change of wettability was achieved, which was represented by the transition from hydrophilic to superhydrophobic surface behavior. The self-assembly ability of n-hexatriacontane resulted in an increased contact angle in all observed samples.

Keywords: Superhydrophobic coating; Contact angle; Wood protection; European oak; Larch; Pine

Contact information: a: Faculty of Forestry and Wood Technology, Department of Furniture, Design and Habitation, Mendel University in Brno, Zemědělská 1, Brno, 613 00, Czech Republic; b: Faculty of Architecture, Institute of Interior and Exhibition Design, Slovak University of Technology in Bratislava, Námestie Slobody 19, 812 45 Bratislava, Slovakia; c: Faculty of Chemical and Food Technology, Department of Organic and Synthetic Materials, Slovak University of Technology in Bratislava, Radlinského 9, 812 37 Bratislava, Slovakia
** Corresponding author: vaclav.sprdlik@mendelu.cz*

INTRODUCTION

Wood is the main construction material used in furniture manufacturing. Currently, wood is used in various forms, *e.g.*, solid wood, laminated wood (plywood, *etc*.) and agglomerated wood-based materials (chipboards, MDF, *etc*.) as well as in combination with other materials.

Solid wood is still utilized in furniture construction thanks to its great mechanical properties, accessibility, low price, and high aesthetic value. Research has established that sanded solid wood without coating is a material with the higher contact comfort in comparison to other standard materials used by interior furnishings (Kotradyova and Teischinger 2012). When coatings are taken into account, the most favorable is a finish with natural waxes and oils (Kotradyova and Teischinger 2014). Unfortunately, there are some drawbacks to using wood material. Wood is naturally hygroscopic, *i.e.*, the dimensions change with increasing humidity. With increasing humidity of the material, wood is also prone to pest infestations (fungi, insects) and mold (Rowell 2005). High

humidity is not suitable for furniture joints. Therefore, it is necessary to protect the surface with a coating. The first protective substances were natural waxes and oils, which prevented absorption of water into the wood surface. During the 20th century, artificial protective films with organic solvents were synthesized to give the surface a higher quality coating. Currently, there is an effort to use more ecologic water-based coating systems, which have lower impact on humans and nature (Bulian and Graystone 2009).

During all the years of development, nature invented its own coating systems, which are 100% organic. These substances are very sophisticated combinations of compounds protecting plants and animals against the external environment. Hydrophobic surfaces can be found on the leaves of many plants and on the feathers of birds. For example, the hydrophobic behavior of the lotus leaf (*Nelumbo nucifera*), which gave its name to the Lotus effect, exhibits superhydrophobicity and self-cleaning properties. This effect is based on a combination of leaf morphology and a blend of waxes deposited on the surface. One of the requirements for superhydrophobicity is the hierarchical structure on the leaf, *i.e.*, the presence of micro- and nano-scale bumps. Microbumps are represented by leaf morphology and nanobumps by a deposited wax blend known as an epicuticular. This behavior is called roughness-induced superhydrophobicity (Nosonovsky and Rohatgi 2012). Its main characteristics are a very high contact angle over 150° (below as CA), low contact angle hysteresis, and a low tilt angle ($\alpha < 5°$). Tilt angle determines the angle at which a drop of water starts to roll off. The wax crystal self-assembly ability is also unique. Crystals of deposited wax start to grow after deposition onto the surface and create 3D objects such as platelets, tubules, tubes, ribbons, *etc*. (Nosonovsky and Bhushan 2012).

Theoretical models explaining the role of roughness on superhydrophobicity mostly try to define CA by analyzing the forces acting on fluid droplet resting on solid surface surrounded by a gas (Young 1805). The Wenzel and Cassie-Baxter equations depending on the extent of liquid/solid interfacial contact area are being generally used to estimate water CAs on superhydrophobic surfaces. Wenzel determined that when the liquid is in intimate contact with a microstructured surface, θ will change to cos θ_W*,

$$\cos \theta_W^* = r \cos \theta \quad (1)$$

where r is the ratio of the actual area to the projected area (Wenzel 1936). Wenzel's equation shows that microstructuring a surface amplifies the natural tendency of the surface. A hydrophobic surface (one that has an original contact angle greater than 90°) becomes more hydrophobic when microstructured – its new CA becomes greater than the original. The Wenzel regime is usually recognized as homogeneous wetting, since the liquid completely penetrates into the grooves. However under some circumstances, especially the increase of the surface roughness, vapor pockets may be trapped underneath the liquid yielding a composite interface. This heterogeneous wetting is usually described by the Cassie-Baxter (CB) model, from which the apparent contact angle (θ_{CB}) is given by equation (Cassie and Baxter 1944):

$$\cos \theta_{CB} = f_s(\cos \theta_c + 1) - 1 \quad (2)$$

According to Eq. 2, droplets will have a higher apparent CA if less area is in contact with the solid substrate. The CB equation simply indicates that the CA can be increased even when the intrinsic contact angle of a liquid on the original smooth surface is less than 90°. However, new developments show that other considerations for CA and CA hysteresis may need to be taken as well. Gao and McCarthy suggested that the contact line model is better

approach to predict superhydrophobicity of surfaces (Gao and McCarthy 2007, 2009). They state that wettability (advancing and receding contact angles, and thus hysteresis) is a function of the activation energies that must be overcome in order for contact lines to move from one metastable state to another. Contact areas play no role in this. Wenzel's and Cassie's equations are valid only to the extent that the structure of the contact area reflects the ground/state energies of contact lines and the transition states between them.
There have been published several studies of hydrophobic plant wax applied to flat artificial surfaces (glass, silicon wafers, and gold plates), replicas of plant leaves, or artificial substrates with microstructures (Koch *et al*. 2009a; Niemietz *et al.* 2009; Cao 2010; Guo and Wang 2010; Bhushan and Jung 2011; Pechook and Pokroy 2012).

The study of Wang *et al*. (2013) showed combined effects of the spherical silica nanoparticles (roughness increment) and their hydrophobization with HDTMS as a promising approach for surface treatment of wood. The first step was growing nanofilms on wood on the basis of a silica sol-gel process; in the second step, the film was modified by the hydrophobic hexadecyltrimethoxysilane (HDTMS). The presented two-step treatment provides Chinese fir with a high hydrophobicity with water, with CAs between 141 ° (longitudinal surface) and 150 ° (transverse surface).

In the more recent study of Tu *et al.* (2016), mechanically robust superhydrophobic surfaces were fabricated on naturally micro-grooved wood based on a two-step process, *i.e*., first applying a primer coating of transparent epoxy resin to cover the surface microstructures, followed by construction of superhydrophobic films followed by construction of superhydrophobic films using silica/epoxy resin/fluorinated alkylsilane (FAS) nanocomposites. The properties of this surface suggest its potential use in various practical applications.

Increased hydrophobicity of the wood was also found on beech wood activated with low temperature atmospheric DCSBD plasma (Jablonsky *et al.* 2016). The hydrophobic effect evolved on plasma activated surfaces during the storage time, mostly on samples which had not been in direct contact with plasma discharge during the treatment. The chemical reaction responsible for hydrophobization of wood samples takes place in a post-discharge zone, which is 5 to 8 mm under the plasma discharge. Combination of plasma discharge and thin film deposition was presented also in a study by Xie *et al.* (2015). The described technique led to a superhydrophobic behavior of wood surface.

The present study, however, uses wood, which is a natural, renewable, and widely used material, as a substrate and natural wax as a coating material. Wood is a composite structure consisting mainly of cellulose, hemicelluloses, and lignin. The surface of wood is easily machinable, and it is very easy to prepare a surface with the required roughness. As mentioned above, surface roughness might be essential for superhydrophobicity. The thin wax coating on the surface of the wood can protect the wood from water penetration or eliminate water penetration into the wood structure, thereby indirectly eliminating the conditions suitable for living organisms. By extension, such a super-thin protective layer does not change the texture of the wood surface in tactile terms and thus contributes to the preservation of the natural character of wood, which is the main goal of this study.

EXPERIMENTAL

Wood Substrate and Microstructure Template

For this experiment, 3 wood species were chosen: European oak (*Quercus robur)*, European larch (*Larix decidua*), and Scots pine (*Pinus sylvestris*). European oak is widely used in the furniture industry due to its durability and strength. Pine is one of the most used species due to its low weight, high strength, low price, and accessibility. Larch is mostly used for house facades, windows, doors, and interior decorations. All species were kiln dried to a humidity of 8 ± 2%, which is standard for furniture manufacturing. All samples were prepared from radial cuts. For this study, 2 sample categories were prepared as follows: (1) 10 ×10 × 5 mm (L ×R × T) for SEM scanning and confocal microscopy; and (2) 60 × 20 × 10 mm (L × R × T) for contact angle and tilt angle measurements. Samples were stored 7 days under the following conditions: temperature (*T*) = 23°C and relative humidity (RH) = 60% until an equilibrium moisture content was reached according to the standard guide for moisture conditioning of wood and wood-based materials ASTM 4933-99. To create a microstructure as the base for a hierarchical structure and the consequent investigation of the roughness dependence of deposited wax, 3 different surface modifications were manufactured as follows: (1) surface brushing with sandpaper roughness 150 (Pine 150, Oak 150, Larch 150); (2) surface planing (Pine P, Oak P, Larch P); and (3) microtome cut with a precision of 0.2 mm (Pine MT, Oak MT, Larch MT). Prior to n-hexatriacontane deposition, all samples were cleaned with pressurized air to avoid the presence of dirt on the surface of samples.

Nanostructure

A wax nanostructure was created by using the alkane n-hexatriacontane ($CH_3(CH_2)_{34}CH_3$) (98% purity, obtained from Sigma-Aldrich, Germany). This substance is capable of self-assembly (Bhushan *et al.* 2009).

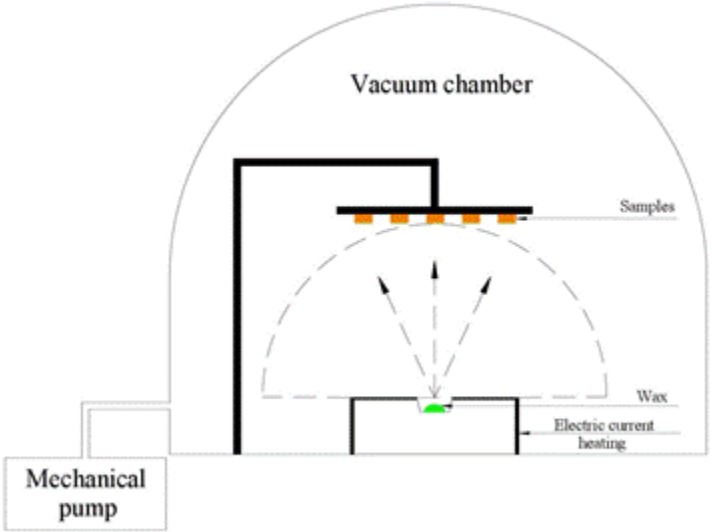

Fig. 1. Diagram of a thermal evaporation system. A box containing wax is heated with pulses of electric current. The wax is melted and evaporated in the hemispherical range onto the samples located above.

After depositing on the surface, molecules of the coating grow and form various 3D objects. These long chain alkanes are common compounds in the epicuticular waxes of hydrophobic plant leaves (Jeffree 2006). When deposited on a smooth surface, n-hexatriacontane causes large contact angles and low tilt angles for water droplets (Tavana *et al.* 2006).

Conditioned wood samples were placed in a vacuum chamber 200 mm above a wax container loaded with $m = 1.12 \pm 0.003$ g of n-heaxatriacontane (Fig. 1). The wax was evaporated at a temperature (T) of 200 °C by applying pulses of an electric current. The temperature of wax evaporation was obtained from experimental study of Pechook and Pokroy (2012). The pressure in the chamber was 10^{-4} mbar. In this case, evaporation occurred in the hemispherical region with a point source where the radius is the distance between the container with wax and the samples. The amount of sublimated mass by surface area was calculated by the amount of the wax in the container divided by surface area (Bhushan *et al*. 2009). The calculated mass of the evaporated wax was about 10 μg/cm^2.

The layer thickness of depisted wax varied between 260 nm and 300 nm. The melting temperature of n-hexatriacontane is $T = 76$ °C, and the wax doesn´t decompose (Matacotta and Ottaviani 1995). Methods of wax evaporation were obtained from the studies of (Pechook a Pokroy 2012; Bhushan *et al.* 2009).

Subsequent SEM observations established that wax crystals create uniform layer regarding the size of the platelets and their growth. According to SEM observation of uncoated samples, it is possible to observe bumps in micrometer scale. The roughness of the surface was much higher than that of the deposited wax layer. After deposition, samples were stored in air-conditioned chambre at 25 °C with humidity 60% except the time when they were measured.

Surface Investigation

The growth of wax crystals was observed with scanning electron microscopy (SEM) at 0 h after deposition of the wax and again after 24 h, 48 h, 72 h, and 96 h of the ageing process. Surface investigation started immediately after wax deposition (0 h). For the SEM investigation, samples were mounted on a holder with double-sided tape and coated with 10 nm of gold by a sputter coater (Type Q150R, Quorum Technologies Ltd., Laughton, UK). A Tescan scanning electron microscope (MIRA3 with Atlas software, Tescan Orsay Holding, Brno, Czech Republic) was used to investigate the wax self-assembly. Observations were made at 15 kV acceleration voltage. Samples dedicated to the self-assembly investigation on SEM were coated with gold prior to observation to facilitate elimination of the possible impact of a cold layer on the wax self-assembly process.

The self-assembly process was investigated with confocal laser microscopy (CLM) at 0 h after the deposition of the wax and again after 24 h, 48 h, 72 h and 96 h. An Olympus LEXT OLS4000 3D laser measuring microscope was used at 50× magnification over a scanned area of 256 × 256 μm.

Contact Angles

The wettability of the wood samples with deposited wax was measured 0 h after deposition of the wax and 24 h, 48 h, 72 h, and 96 h incrementally thereafter. The sample dimensions were 60 × 20 × 10 mm. During ageing, a new series of samples was used every day. The static contact angle was measured (Advex Instruments, Brno, Czech Republic)

and calculated with SeeSystem 6.3 software. For wettability measurements, 5 µL drops of demineralized water were used. Reference samples with no wax layer were also measured.

RESULTS AND DISCUSSION

SEM Observation

Images from SEM show different processes of wax crystal growth between coniferous (pine and larch) and deciduous (oak) species. There was also a difference between the structures developed on the surfaces of pine and larch. The surface finish of the samples had an impact on the formation and shape of crystal. The difference was observed during the self-assembly process and contact angle measurements. Figure 2 depicts all species without any coating prepared with a Microtome cut. It shows a smooth surface without any sign of platelets of other 3D objects.

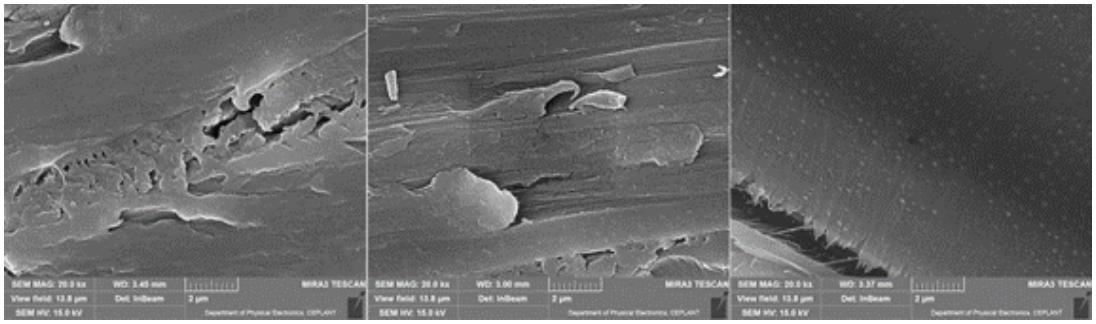

Fig. 2. Samples of microtome cut without coating. Let to right: European larch, European oak and Scots pine

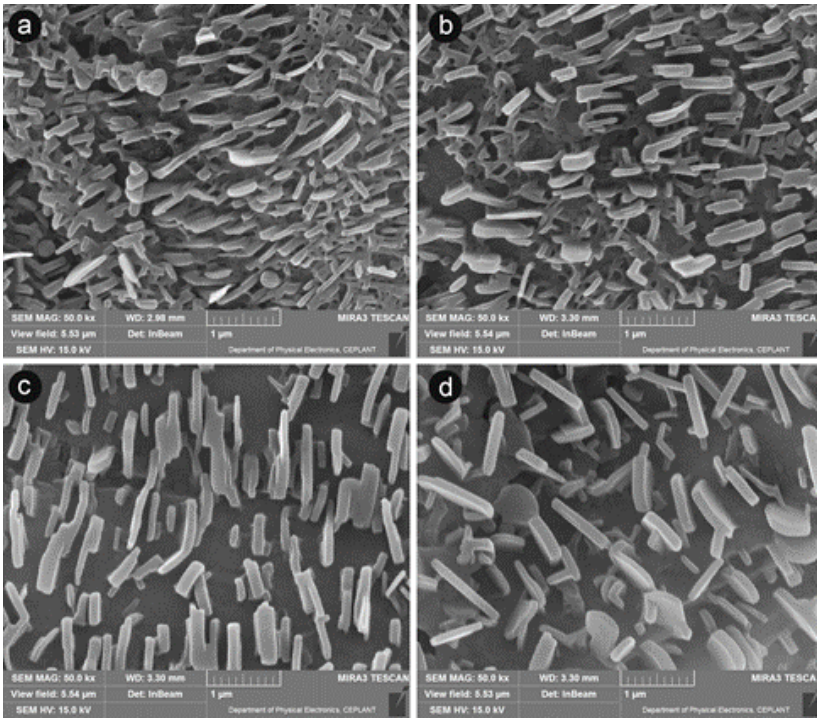

Fig. 3. Self-assembly of deposited n-hexatriacontane on European oak (*Quercus robur*) prepared with a microtome at a) 0 h, b) 24 h, c) 48 h, and d) 96 h after wax deposition

European Oak

In the case of oak 150, the surface was covered by small platelets (200 × 50 × 200 nm) that were connected to each other on random places with no free-standing platelets. This structure looks like a net (Fig. 2). This net served as a reservoir for the wax during the self-assembly process; there was remarkable growth of bigger and separated platelets. The length, width, and height varied from 700 to 1000 nm, 100 to 300 nm, and 400 to 600 nm, respectively. The growth of the crystals was perpendicular to the surface even on places that were not horizontal (vessels, imperfections due to surface finish). Images after 96 h exhibited considerable connections between the platelets. The orientation of the 3D platelets along the Y and X axes was random. Surface treatment by milling and by microtome cut resulted in some exceptions on the surface. Locally, the large platelets described previously as well as small platelets (approximately 200 × 50 × 200 nm) were observed. Depending on the surface roughness, there were differences between the growth of the crystals, resulting in a "melted" structure.

European Larch

In larch, platelets and local fissures (in tracheids) were created (Fig. 4). On the first day of observation, self-assembly started from the net of small platelets that were connected to each other in various ways. Small platelets gradually grew into larger ones, leaving an increasing number of free spaces on the surface. Orientation along the X and Y axes was random. Orientation along the Z axis was not strictly perpendicular to the surface; some platelets were folded in various angles up to 45° against the surface. The shape of the platelets was more geometric than those on oak (Fig. 3).

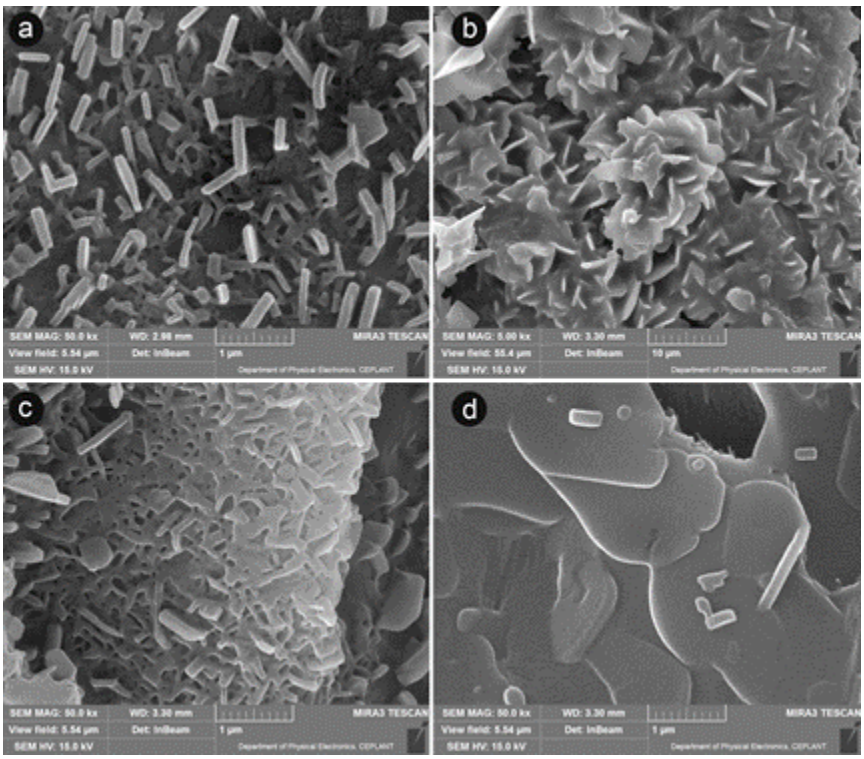

Fig. 4. Various wax crystal modifications observed during self-assembly on the surface of European larch (*Larix decidua*). a) Large connected platelets and relics of indigenous net, b) flower-like object, c) "melted" structure of the wax, and d) fissures of wax with small platelets

A new flower- shaped 3D object occurred locally on the surface during scanning after 48 h following deposition. Figure 3 depicts exceptions that occurred during the observations; the regular behavior was similar to that of European oak.

Scots Pine

The self-assembly process started with an almost flat layer with small bumps for samples brushed with sandpaper 150. In approximately 10% of scans, larger structures appeared as flower-like crystals (3 to 5 µm) with small bumps on the wax surface. The first category had an organic structure, while the second appeared more like a cluster of lenticular platelets where the direction and place of conjunction was random. Some areas of the sample were covered with a thin film of wax for the whole time of scanning, and the self-assembly process did not result in a 3D object but in a flat film with fissures. This phenomenon is caused by different chemical composition of wood through the cuts

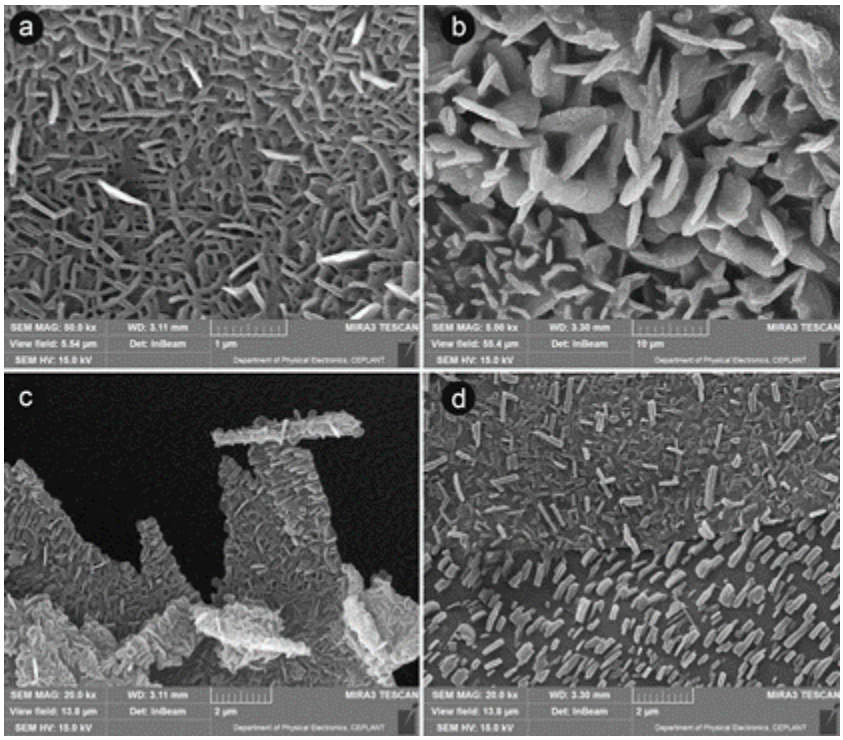

Fig. 5. Various wax crystal modifications observed during self-assembly process on the surface of Scots pine (*Pinus sylvestris*). a) Dense network of deposited wax, b) flower-like lenticular platelets, c) surface imperfection covered with wax platelets, and d) wax platelet interface between wood and resinous channel

For the planed samples, self-assembly created standard platelets and giant wax structures, which manifested in the form of flower-like shapes and clusters of lenticular platelets. The flower-like objects were covered with smaller bumps of wax. Regular platelets had dimensions similar to those mentioned above. Between platelets, there were smaller objects that were relics of the indigenous net. In the microtome cut samples, the net consisted of small and short objects (platelets, tubules). Locally, the wax layer was a thin film with smaller bumps. At 48 h after deposition, large structures that were flower-like lenticular platelets of a cluster shape appeared. These large structures were covered with small bumps (500 to 1000 nm). Regular platelets were connected at their lateral ends.

The various 3D objects are shown in Fig. 5. The regular behavior of the self-assembly process was comparable to European oak and European larch.

The formation and the process of wax crystal creation is described well in several papers (Bhushan *et al*. 2009; Pechook and Pokroy 2012). However, these studies focused only on the process of wax self-assembly on inert and flat surfaces. N-hexatriacontane usually forms platelets, and these objects are created over time (Bhushan 2011). Currently there are no available studies dealing with the creation of crystals on organic substrates, nor of the dependence that crystal growth has on surface roughness. Pechook and Pokroy (2012) studied surfaces with n-hexatriacontane and noted that over 160 h, crystals grew from 50 nm to 800 nm. Furthermore, a film of wax was created, and after 96 h, wax crystals ranged from 1000 to 1500 nm. The growth of the wax structures is gradual and forms a 3-D structure (Dorset *et al*. 1983). The observed structures are comparable with structures on plant leaves, *e.g*., *Convalaria majestis*, *Colocasia esculenta*, and *Triticum aestivum* (Koch *et al*. 2006; Koch *et al.* 2009b). Due to the composite character of wood and chemically diverse (natural) character of the wood surface, unexpected structures appeared on the surface. Chemical These structures were ridged rodlets on *Willimdendron* and fissures on *Crassula ovata* (Koch and Ensikat 2008; Koch *et al*. 2009b).

Remarkable changes in the size and type of the crystals are most likely caused by the extractive compounds of wood, chemical reactions between the wood surface and wax, and differing porosity in various areas of the sample. Wood is a complex and inhomogeneous material, and different species exhibit different self-assembly behaviors.

Confocal Microscope Measurements

Scanning by confocal microscope was performed to verify the self-assembly ability of n-hexatriacontane on wood surfaces with differing roughness (Fig. 6).

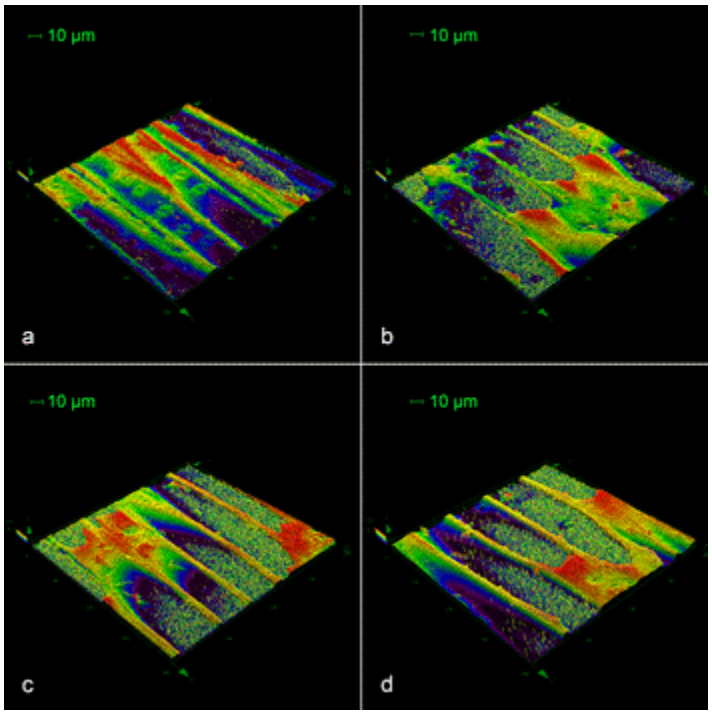

Fig. 6. Confocal scanning of deposited n-hexatriacontane. a) Reference sample without wax and samples of European larch *(Larix decidua)* prepared with a microtome after self-assembly for b) 48 h, c) 72 h, or d) 96 h

Samples were prepared by surface brushing with sandpaper roughness 150, surface planing and microtome cut with a precision of 0.2 mm. Measurements were done immediately after deposition of the wax (0 h) and 24 h, 48 h, 72 h, and 96 h after the self-assembly process. Scanning confirmed the gradual growth of wax crystals, with the best results observed on samples modified with a microtome cut in vessels and tracheids. There were no signs of structures on reference samples, where the surface was not coated with n-hexatriacontane.

On subsequent scans immediately after wax deposition, the growth of crystals was obvious. Development of the wax structure was gradual, and the process was represented by peaks in the z axis. The height of peaks was approximately 10 µm but varied due to the uneven distribution of the wax during deposition. Differences between the species were not remarkable due to the high roughness of the surface, which limited the magnification. Differences between the reference sample and scans made after 96 h of self-assembly are shown in Fig. 6.

The depicted samples are from the European larch prepared by microtome cut. The samples of oak and pine exhibited similar results during their self-assembly process. However, larch samples showed the most remarkable changes during crystal growth. The effects of the self-assembly process are represented by growing peaks of wax crystals in the blue and violet parts of the sample (smooth inner walls of tracheids and vessels in the tangential direction). The gradual filling of the wood structure is expressed by a color change to green.

Contact Angle Measurements

The influence of the wax layer on wettability was observed by measuring contact angle (CA) and tilt angle (Table 1). All wood species exhibited changes in the contact angle, with remarkable differences occurring between the pine and the group of larch and oak. Tilt angle measurements were performed for samples with still water droplets. In this case, the tilt angle was 90°, and the droplets still adhered to the surface. Exceptions are mentioned below. Reference samples with surface treatment were measured for all sample categories. Result of reference samples were generalized for each species, since the differences were in range of standard deviation.

European oak

The samples measured at 0 h exhibited hydrophobic behavior. The CA of oak samples was 138° for Oak 150, 140° for Oak planed, and 137° for Oak MT. The same phenomenon as with larch occurred during the oak measurements. Superhydrophobicity was observed during contact angle measurements, same as with larch samples. Some samples were so hydrophobic that it was not possible to retain a drop on the surface. Roll-off happened immediately after the drop touched the surface, so measuring was not possible.

The samples were labeled as fully hydrophobic (superhydrophobic). Nevertheless, even without counting the fully hydrophobic samples, other samples also achieved superhydrophobic properties. The mean contact angles after 96 h of self-assembly were as follows: Oak MT, 153°; Oak planed, 160+°; and Oak 150, 150°. Self-assembly impacts on the contact angles are depicted in Fig. 6.

Table 1. Contact Angle Measurements

Time after deposition [h]	0	24	48	72	96	Increase of CA [%]
Pine 150	130 ± 6.5	131 ± 3.8	138 ± 3.5	141 ± 3.8	142 ± 2.9	9.2
Pine p	123 ± 3.0	124 ± 2.6	126 ± 4.0	132 ± 3.8	139 ± 3.9	12.5
Pine MT	136 ± 2.6	136 ± 4.9	138 ± 4.3	138 ± 2.3	141 ± 1.3	3.6
Pine ref	80 ± 4.6	80 ± 4.6	80 ± 4.6	80 ± 4.6	80 ± 4.6	
Larch 150	135 ± 3.9	144 ± 0.0	140 ± 0.8	150 ± 0.0	150 ± 1.3	11.7
Larch p	134 ± 4.2	141 ± 4.9	139 ± 5.2	140 ± 3.4	152 ± 5.2	13.6
Larch MT	136 ± 2.9	144 ± 0.9	141 ± 3.2	147 ± 3.8	150 ± 1.3	10.2
Larch ref	53 ± 4	53 ± 4	53 ± 4	53 ± 4	53 ± 4	
Oak 150	138 ± 1.3	140 ± 0.0	149 ± 2.7	150 ± 0.0	151 ± 1.7	9.1
Oak p	140 ± 1.4	135 ± 6.3	142 ± 1.0	146 ± 2.8	150 ± 0.0	7.3
Oak MT	137 ± 3.5	146 ± 4.8	150 ± 0.0	150 ± 0.0	153 ± 0.5	11.4
Oak ref	69 ± 9.5	69 ± 9.5	69 ± 9.5	69 ± 9.5	69 ± 9.5	

Note: Data shown are averages ± standard deviation:

European larch

The samples measured at 0 h exhibited hydrophobic behavior. The CA from day 0 was 135° for Larch 150, 133° for Larch planed, and 136° for Larch MT. During measurement of the larch samples an unexpected phenomenon occurred; some samples were so hydrophobic that it was not possible to retain a drop on the surface. After placing the drop on the surface, the drop immediately rolled off, so that it was not possible to measure the contact angle. However, several drops were retained and measured. Thus, these samples were labeled as fully hydrophobic (superhydrophobic). If experiments with unmeasurable CA were not counted, the surface behavior achieved superhydrophobic properties, *i.e*., CA more than 150 °, as follows: Larch MT, 150°; Larch planed, 152°; and Larch 150, 150°.

Scots pine

Samples measured 0 h after wax deposition showed the following results: Pine 150, 127°; Pine MT, 137°; and Pine planed, 123°. Although all surfaces exhibited hydrophobic behavior, rolling of the drops did not occur. Even at a tilt angle 90°, the water drop did not roll off. After 96 h, the self-assembly process led to increased contact angles, as follows: Pine 150, 142°, Pine MT, 141°, Pine planed, 139°. Microtome surfaces exhibited the lowest increase of the contact angle for 5°. Nevertheless, a CA of 141° is a still highly hydrophobic surface. Sanded and planed surfaces exhibited increases in CA of about 15°, and the increase developed continuously over time.

Samples in this study were stored under similar conditions (25 °C) as previously described (Niemietz *et al*. 2009), but they exhibited higher contact angles (CA > 150°).

The contact angles of larch and oak became superhydrophobic after 96 h of self-assembly, while pine achieved similar results as previously described (Niemietz *et al.* 2009). Pechook and Pokroy (2012) found contact angles higher than 160°, but the temperature of storage was higher, leading to chemical reactions in the wax structure (Niemietz *et al.* 2009). During the contact angle measurement (larch, pine), an unexpected phenomenon occurred. Some areas of the sample were superhydrophobic, and some only hydrophobic with a difference of approximately 15°, which could not be attributed to measurement errors. It was most likely caused by the reaction between the resin in the wood and the wax. It was assumed that areas more saturated with resin are more hydrophobic.

Niemietz *et al.* (2009) and Bhushan *et al.* (2009) stated that samples stored at 25 °C with deposited wax had a tilt angle of 90°. The same results were obtained during this study; even when the samples were tilted to 90°, a drop of water still adhered to the surface. Considering this phenomenon, surfaces observed in this study can be claimed as hydrophobic surfaces with hierarchical structure (micro- and nano-structures), as described by Wenzel (1936) and Cassie and Baxter (1944). It can be assumed that these samples were in the Wenzel wetting state, *i.e.*, water drops penetrate the structure and are pinned to the surface, which leads to higher adhesion (Wenzel 1936; Cassie and Baxter 1944).

CONCLUSIONS

1. By depositing n-hexatriacontane onto lark and oak surfaces, superhydrophobic surface behavior was achieved. The surface of pine wood was only highly hydrophobic.
2. The self-assembly process decreased wettability (increases hydrophobicity) but increased the contact angle from 5° to 12° depending on the species and surface roughness.
3. The highest contact angles were achieved on surfaces prepared with a microtome cut. Comparing reference samples and samples with deposited wax, the highest increase was observed in larch, where the CA_{ref} was only 53°; after wax deposition, the CA increased up to 150°. The CA of pine increased from 79° to around 140° depending on surface roughness, while the CA of oak increased from 70° to 150°.
4. Development of hydrophobicity caused by the wax on the wood surface was gradual and required at least 4 days. Longer periods were not measured, but, from the measurements of contact angles on samples sanded with 150 sandpaper, it was obvious that after 3 days, CA reached an equilibrium that does not change remarkably thereafter.
5. The self-assembly process was verified by confocal microscopy, and several types of crystals were observed using SEM images. This study can be a first step towards innovation in organic coatings of wood, which are considerably more hydrophobic but still environmentally friendly.

ACKNOWLEDGEMENTS

This work was supported by the Slovak Research and Development Agency under contract No. APW-0594-12, Interaction of Wood and Human, Bratislava, Slovak Technical University, Faculty of Architecture, Slovakia, and CEPLANT - R&D Centre for Low-Cost Plasma and Nanotechnology Surface Modifications, Masaryk University in Brno, Czech Republic.

REFERENCES CITED

Bhushan, B. (2011). "Biomimetics inspired surfaces for drag reduction and oleophobicity/philicity," *Beilstein Journal of Nanotechnology* 2, 66-84.

Bhushan, B., and Jung, Y. C. (2011). "Natural and biomimetic artificial surfaces for superhydrophobicity, self-cleaning, low adhesion, and drag reduction," *Progress in Materials Science* 56(1), 1-108. DOI: 10.1016/j.pmatsci.2010.04.003

Bhushan, B., Koch, K., and Jung, Y. C. (2009). "Fabrication and characterization of the hierarchical structure for superhydrophobicity and self-cleaning," *Ultramicroscopy* 109(8), 1029-1034. DOI: 10.1016/j.ultramic.2009.03.030

Bulian, F., and Graystone, J. A. (2009). *Wood Coatings: Theory and Practice*, Elsevier, Amsterdam, Netherlands.

Cao, L. (2010). *Superhydrophobic Surface Design Fabrication and Application*, Ph.D. Dissertation, University of Pittsburgh, Pittsburgh, PA, USA.

Cassie, A. B. D., and Baxter, S. (1944). "Wettability of porous surfaces," *Transactions of the Faraday Society* 40(5), p.546.

Gao, L., and McCarthy, T. J. (2007). "How Wenzel and Cassie were wrong," *Langmuir* 23, 3762-3765.

Gao, L., and McCarthy, T. J. (2009). "An attempt to correct the faulty intuition perpetuated by the Wenzel and Cassie "Laws"," *Langmuir* 25, 7249-7255.

Guo, Y., and Wang, Q. (2010). "Facile approach in fabricating superhydrophobic coatings from silica-based nanocomposite," *Applied Surface Science* 257(1), 33-36.

Jablonský, M., Šmatko, L., Botkova, M., Tino, R., and Šima, J. (2016). "Modification of wood wettability (European beech) by diffuse coplanar surface barrier discharge plasma," *Cellulose Chem. Technol.* 50(1), 41-48 (2016).

Jeffree, C. E. (2006). "The fine structure of the plant cuticle," in: *Annual Plant Reviews Volume 23: Biology of the Plant Cuticle*, Blackwell Publishing Ltd, Oxford, UK. pp. 11-125. DOI: 10.1002/9780470988718.ch2

Koch, K., Barthlott, S., Koch, S., Hommes, A., Wnadelt, K., Mamdouh, S., De-Feyter, S., and Broekmann, P. (2006). "Structural analysis of wheat wax (*Triticum aestivum*, c.v. "Naturastar" L.): from the molecular level to three dimensional crystals," *Planta* 223(2), 258-270. DOI: 10.1007/s00425-005-0081-3

Koch, K., Dommisse, A., Niemietz, A., Baarthlott, W., and Wandelt, K. (2009a). "Nanostructure of epicuticular plant waxes: Self-assembly of wax tubules," *Surface Science* 603(10-12), 1961-1968.

Koch, K., Bhushan, B., and Barthlott, W. (2009b). "Multifunctional surface structures of plants: An inspiration for biomimetics," *Progress in Materials Science* 54(2), 137-178. DOI: 10.1016/j.pmatsci.2008.07.003

Koch, K., and Ensikat, H. J. (2008). "The hydrophobic coatings of plant surfaces: Epicuticular wax crystals and their morphologies, crystallinity and molecular self-assembly," *Micron* 39(7), 759-772.

Kotradyova, V., and Teischinger, A. (2012). "Aestetic performance of different wood species - Visual interaction of human being and wood (by analizing the colour and the texture of wood separately)," *Innovation in Woodworking Industry and Engineering Design* 1, 25-30.

Kotradyova, V., and Teischinger, A., (2014). "Tactile interaction and comfort of wood materials interaction of human and wood," in: *57th International Convention of the Society of Wood Science and Technology (SWST)*, Zvolen, Slovakia, (http://www.swst.org/meetings/AM14/pdfs/presentations/kotradyova pdf.pdf).

Matacotta, F. C., and Ottaviani, G. (1995). "Science and technology of thin film," River Edge, N.J.: World Scientific publishing Co. Article submitted: May 12, 2016;

Niemietz, A., Wandelt, K., Barthlott, W., and Koch, K. (2009). "Thermal evaporation of multi-component waxes and thermally activated formation of nanotubules for superhydrophobic surfaces," *Progress in Organic Coatings*, 66(3), 221-227.

Nosonovsky, M., and Bhushan, B. (2012). *Green Tribology: Biomimetics, Energy Conservation and Sustainability*, Springer, New York, NY.

Nosonovsky, M., and Rohatgi, P. K. (2012). *Biomimetics in Materials Science*, Springer, New York, NY.

Pechook, S., and Pokroy, B. (2012). "Self-assembling, bioinspired wax crystalline surfaces with time-dependent wettability," *Advanced Functional Materials* 22(4), 745-750.

Rowell, R. (2005). *Handbook of Wood Chemistry and Wood Composites*, CRC Press, Boca Raton, FL, USA.

Tavana, H., Amirfazli, A. M., and Neumann, A. W. (2006). "Fabrication of superhydrophobic surfaces of n-hexatriacontane," *Langmuir* 22(13), 5556-9. DOI: 10.1021/la0607757

Tu, K., Wang, X., Kong, L., Chang, H., and Liu, J. (2016). "Fabrication of robust, damage-tolerant superhydrophobic coatings on naturally microgrooved wood surfaces," *RSC Advances* 6, 701-707. DOI: 10.1039/c5ra24407b ;

Wang, X., Chai, Y., and Liu, J. (2013). "Formation of highly hydrophobic wood surfaces using silica nanoparticles modified with longchain alkylsilane," *Holzforschung* 67(6), 667-672. DOI: 10.1515/hf-2012-0153

Wenzel, R. N. (1936). "Resistance of solid surfaces to wetting by water," *Journal of Industrial and Engineering Chemistry* 28, 988-994.

Xie, L., Tang, Z., Jiang, L., Breedveld, V., and Hess, D. W. (2015). "Creation of superhydrophobic wood surfaces by plasma etching and thin-film deposition," *Surface & Coatings Technology* 281, 125-132.

Young, T. (1805). "An essay on the cohesion of fluids," *Phil. Trans. R. Soc. Lond*. 95, 65-87. DOI:10.1098/rstl.1805.0005

Article submitted: May 12, 2016; Peer review completed: July 30, 2016; Revised version received and accepted: February 20, 2017; Published: March 17, 2017.
DOI: 10.15376/biores.12.2.3289-3302